Tribological Behavior of γ-TiAl Matrix Composites with Different Contents of Multilayer Graphene

Zhao Yan, Qiao Shen, Xiaoliang Shi, Kang Yang, Jialiang Zou, Yuchun Huang, Ao Zhang, Ahmed Mohamed Mahmoud Ibrahim, and Zhihai Wang

In this study, the effect of friction layer thickness and subsurface nano-hardness of wear track on tribological behavior of γ-TiAl matrix composites is investigated. The results of dry sliding tribolocial tests of γ-TiAl matrix composites with 0-2.25 wt.% multilayer graphene (MLG) (0.25 wt.% in tolerance) under different applied loads are reported. The testing results show that the optimized addition amount of MLG is 1.75 wt.% at 12 N (friction layer thickness 3.23 μm, subsurface nano-hardness of wear track 9.03 GPa). It can be found that a continuous and thick friction layer is formed in γ-TiAl-1.75 wt.% MLG at 12 N, resulting in a lower friction coefficient of 0.31 and wear rate of 2.09×10^{-5} mm^3 N^{-1} m^{-1}. During dry sliding process, the high subsurface nano-hardness of wear track leads to the increase in resisting plastic deformation capacity and reduces the material loss. Meanwhile, the thick friction layer contains MLG with high tensile strength which is easily sheared off. Hence, γ-TiAl matrix composites show excellent tribological performance of a friction-reducing and an increase in wear resistance. The investigation shows that γ-TiAl-1.75 wt.% MLG, due to its excellent tribological behavior at 12 N, can be chosen as a promising structural material for minimizing friction- and wear-related mechanical failures in sliding mechanical components.

1. Introduction

In recent years, energy-reducing and material-saving is one of the greatest challenges in the moving mechanical assemblies of γ-TiAl-based alloys. The objective of improving tribological behaviors of γ-TiAl-based alloys is to further enlarge their applications in the engineering field of aerospace and automobile industries. An effective method of improving the properties of anti-friction and wear resistance of γ-TiAl-based alloys by adding solid lubricants was proposed (Ref 1, 2).

In the search for the perfect lubricant which provides the low friction and wear, multilayer graphene (MLG), a crystallographically perfect film of graphitic carbon, has been investigated. The typical images of hexagon and multilayer molecular structure of MLG are shown in Fig. 1. As shown in Fig. 1(a), (b), MLG with the two-dimensional hexagon structure derives from many single-layered sheets of graphite, which might not only cause low wear but also provide easy shearing. In consequence of the prominent combination of tribological properties (Ref 3), mechanical and thermal behaviors (Ref 4-7), MLG is a promising solid lubricant to improve the sliding

Zhao Yan and Qiao Shen have contributed equally to this work.

Zhao Yan, Qiao Shen, Xiaoliang Shi, Kang Yang, Jialiang Zou, Yuchun Huang, Ao Zhang, Ahmed Mohamed Mahmoud Ibrahim, and **Zhihai Wang**, School of Mechanical and Electronic Engineering, Wuhan University of Technology, 122 Luoshi Road, Wuhan 430070, China and Hubei Digital Manufacturing Key Laboratory, Wuhan University of Technology, 122 Luoshi Road, Wuhan 430070, China. Contact e-mail: sxl071932@126.com.
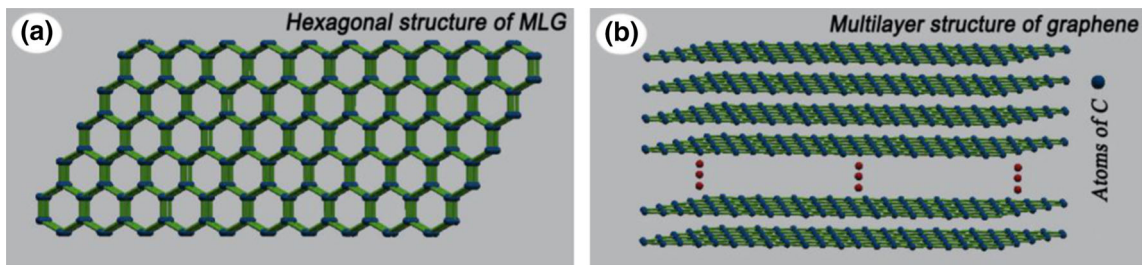
friction and wear behaviors of γ-TiAl-based alloys. MLG has been widely used as reinforcing filler to prevent deformation (Ref 8). In addition, tribological studies also suggest that MLG can be sheared off and welded at a higher load during the sliding wear process, providing a lubricating effect (Ref 9).

Increasing attention has been focused on the research of subsurface nano-hardness and friction layer thickness. The effect of subsurface nano-hardness or friction layer has been widely debated. Xu et al. (Ref 10) studied the formation of friction layer structure with a nano-crystalline structure in MLG-reinforced γ-TiAl matrix self-lubricating composites against Si$_3$N$_4$ ball. The nano-indentation results show that the grain refinement layer when compared with the wear-induced layer has a higher hardness and elastic modulus. This special microstructure of friction layers beneath the surface after sliding leads to the low friction coefficient and high wear resistance of MLG-reinforced γ-TiAl matrix self-lubricating composites. Moreover, it is deduced that the appearance of a nano-crystalline structure results in hardening of the material. Moshkovich et al. (Ref 11) studied the friction and wear of copper in different lubricant regimes, showing that severe plastic deformation of the friction layer under sliding process was correlated with a nano-crystalline structure. In addition, the wear process under the boundary lubrication regime was found to expose fresh metallic regions repeatedly, whereas friction under the elastohydrodynamic lubrication regime led to the formation of uniform friction layers that were responsible for the low friction and wear. Zhai et al. (Ref 12) investigated the formation of friction layers of Ni$_3$Al matrix composites with MLG under different contact loads. The results showed that under 15 N load, the friction layer with an ultrafine grain and nano-crystalline structure mainly consisted of a thin debris re-embedded layer and a matrix refinement layer, which played an important role in improving the tribological properties. Although these works have provided useful information on friction layer and subsurface nano-hardness to a certain extent,

Fig. 1 Typical images of hexagon and multilayer molecular structure of MLG: hexagon structure (a) and multilayer structure (b)
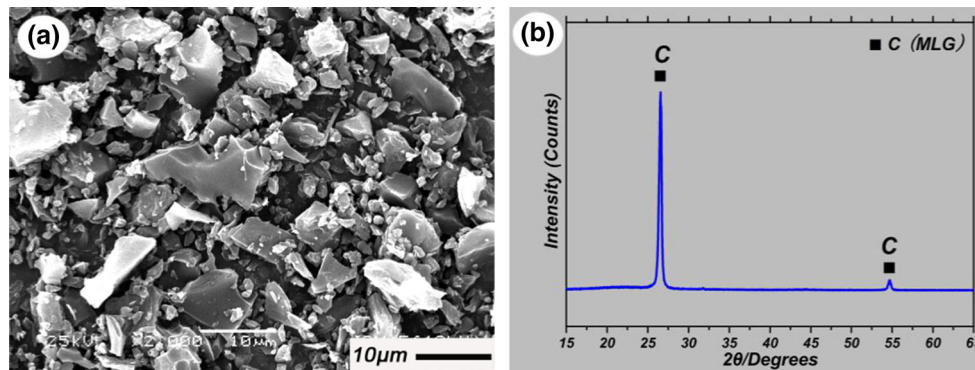

Fig. 2 Typical graph (a) and XRD pattern (b) of MLG powders

the wear mechanisms, subsurface nano-hardness and friction layer thickness of TMSC containing MLG need to be further researched.

In this study, spark plasma sintering (SPS) is adopted to fabricate TMSC containing varied MLG amounts from 0 to 2.25 wt.% (TCM). The sliding tribological tests of TCM are executed for 80 min on the ball-on-disk tribometer of HT-1000 at 4, 8 and 12 N with ambient temperature of 25 °C and a constant speed of 0.2 m/s. With reference to every selected applied load, the addition amount of MLG is optimized to obtain the small friction coefficient and less wear rate. The effect of friction layer thickness and subsurface nano-hardness on tribological behavior of γ-TiAl matrix composites can be studied in detail by four steps: *Step 1* discussing the effect of MLG content on subsurface nano-hardness of wear track (nano-hardness) of TCM; *Step 2* exploring the effect of distributing areas and main existing status of MLG [parallel to wear scar (Para-WS), perpendicular to wear scar (Perp-WS)] on mean nano-hardness of TCM; *Step 3* analyzing the influence of nano-hardness on tribological behavior of TCM; *Step 4* researching the influence of friction layer thickness on tribological behavior of TCM. The above results can enrich the tribological system of self-protection of the MLG-reinforced composites in moving mechanical assemblies.

2. Synthesizing and Testing

2.1 Preparing Technology of TCM

γ-TiAl matrix composites (4 8 at.% Ti-47 at.% Al-2 at.% Cr-2 at.% Nb-1 at.% B) containing the various amounts of MLG from 0 to 2.25 wt.% (0.25 wt.% in tolerance) are fabricated using SPS of D.R. Sinter® SPS3.20 apparatus. Figure 2 presents the typical graph and XRD pattern of MLG. As shown in Fig. 2, the lamellar structure of MLG is clearly distinguished, and MLG powders are very pure. Figure 3(a) exhibits the representative FESEM morphology of MLG. Figure 3(b) shows the magnified micro-morphology of local region marked by rectangle in Fig. 3(a). It is found that this structure has an effect on the tribological properties (Ref 13). Before SPS, the commercially available powders of Ti, Al, B, Nb, Cr (less 20 μm in size, 99.9% in purity) and MLG need to be mixed by vibration milling with a frequency of 45 Hz in Teflon vials. MLG powders were purchased from Nanjing XFNANO Materials Tech Co., Ltd. MLG produced by chemical mechanical stripping method has an average thickness of 40 nm and an average lateral dimension of 50 μm. After being mixed and dried, the powders are adopted to fabricate TCM in graphite molds (25 mm in inner diameter) at 1050 °C with a pressure of 35 MPa for 10 min in protective argon atmosphere. Finally, the as-prepared specimen was ground to remove the surface layer and polished mechanically with successive grades of emery papers down to 1, 200 grit, 5 μm up to a mirror finish.

2.2 Microstructure Analysis

As-prepared TCM specimen and raw MLG powders are studied with Cu-Kα radiation at 30 kV and 40 mA at a scanning speed of $0.01° \text{ s}^{-1}$. The wear scar morphologies are characterized using the electron probe microanalysis (EPMA, JEOL Corporation, Japan) of JAX-8230. The cross-sectional morphologies of TCM specimen and raw MLG powders are analyzed by a field emission scanning electron microscope (FESEM, Zeiss Corporation, Germany) of ULTRA-PLUS-43-13. Nano-hardness is calculated from the load and depth data obtained by nano-indentation in the friction layer and TCM at
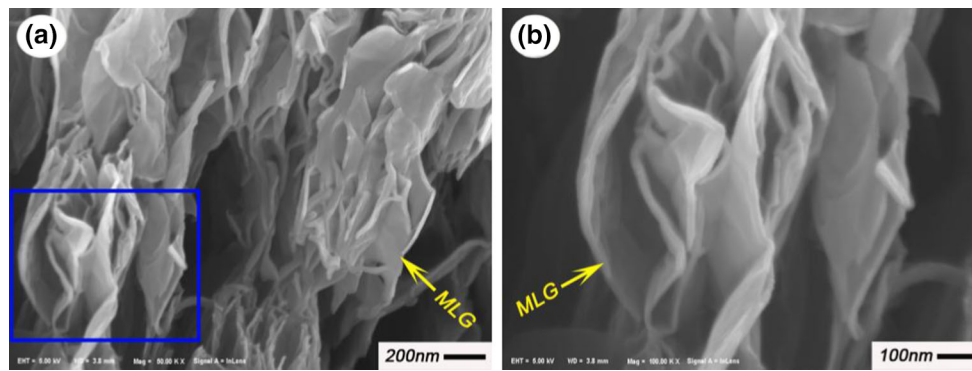
Fig. 3 Representative FESEM morphology of MLG (a) and the high magnification image (b) of the rectangle in (a)

Table 1 Mean and standard deviation of Vicker's hardness and measured density of TCM

Sample	Vicker's hardness		Measured density		
	Mean, GPa	SD	Mean, g/cm^3	SD	Relative density, %
TCM(0 wt.% MLG)	4.79	0.23	3.68	0.030	92.0
TCM(0.25 wt.% MLG)	4.86	0.22	3.74	0.023	93.7
TCM(0.75 wt.% MLG)	5.12	0.18	3.76	0.019	94.6
TCM(1.25 wt.% MLG)	5.34	0.15	3.77	0.015	95.2
TCM(1.75 wt.% MLG)	5.91	0.12	3.80	0.011	96.4
TCM(2.25 wt.% MLG)	4.76	0.23	3.65	0.026	92.9

peak indentation load of 8000 μN using a nano-mechanical test instrument (HYSITRON, Inc.).

2.3 Vicker's Microhardness and Density Measuring

The Vicker's microhardness of TCM samples was measured according to ASTM standard E92-82 [American Society for Testing and Materials (Ref 14)] using a HV1/10 Vicker's hardness instrument. The tests were carried out at three locations to reduce the random errors. The densities of specimens were measured based on Archimedes' principles and according to ASTM Standard B962-08 [American Society for Testing and Materials (Ref 15)]. Eight tests were conducted. The mean and standard deviation of Vicker's hardness and measured density of TCM were given (see Table 1).

2.4 Sliding Friction and Wear Testing

According to ASTM Standard G99-05 (Ref 16), the sliding friction and wear tests of TCM were executed for 80 min on the ball-on-disk tribometer of HT-1000 (Zhong Ke Kai Hua Corporation, China). The test temperature was 25 °C and the applied loads ranged from 4 to 12 N. After being cleaned and dried, TCM disks slid against Si$_3$N$_4$ balls of 6 mm in diameter with a constant sliding velocity of 0.2 m/s at the relative humidity of 65-70%.

2.5 Characterizations of TCM and γ-TiAl-1.75 wt.% MLG

Figure 4(a) shows the typical FESEM morphology of MLG in cross section of γ-TiAl-1.75 wt.% MLG. Figure 4(b) shows the typical magnified morphology of local region marked by rectangle in Fig. 4(a). As shown in Fig. 4(a) and (b), unique bending and folding structures of MLG are easily identified on the fractured surface of TCM. Hence, it can be concluded from

FESEM morphologies of cross section of TCM that the structures of MLG are largely retained after SPS process. As shown in Table 1, the Vicker's hardness of γ-TiAl-1.75 wt.% MLG obtained the optimal values. It can be found that a certain addition amount of MLG improves the microstructure of TCM, and homogeneous lamellar multilayer structure of MLG in γ-TiAl-1.75 wt.% MLG substrate promotes the increase in microhardness of γ-TiAl-1.75 wt.% MLG. Figure 4(c) exhibits the typical XRD pattern of γ-TiAl-1.75 wt.% MLG prepared by SPS. As shown in Fig. 4(c), γ-TiAl-1.75 wt.% MLG is mainly composed of γ-TiAl, MLG and a small amount of TiC according to the intensities of diffraction peaks of existing phases.

3. Results and Analysis

3.1 Friction and Wear Behavior of TCM

During the dry sliding wear test, the friction coefficients are measured and recorded as sliding continues using the control computer system of ball-on-disk tribometer. The wear rate W is determined as Formula 1 (Ref 17):

$$W = \frac{V}{F \cdot L} = \frac{2\pi \cdot R \cdot A}{F \cdot L} \qquad \text{(Eq 1)}$$

where V is the wear volume obtained during the sliding process, F is chosen applied load, L is the sliding distance, and R is the frictional radius. A, the cross-sectional area of wear scar, can be measured using the surface profiler of ST400.

Figure 5 exhibits the representative mean friction coefficients and wear rates of TCM after sliding process. As shown in Fig. 5(a) and (b), it is obvious that the friction coefficients and wear rates decrease to a relatively stable value along with the
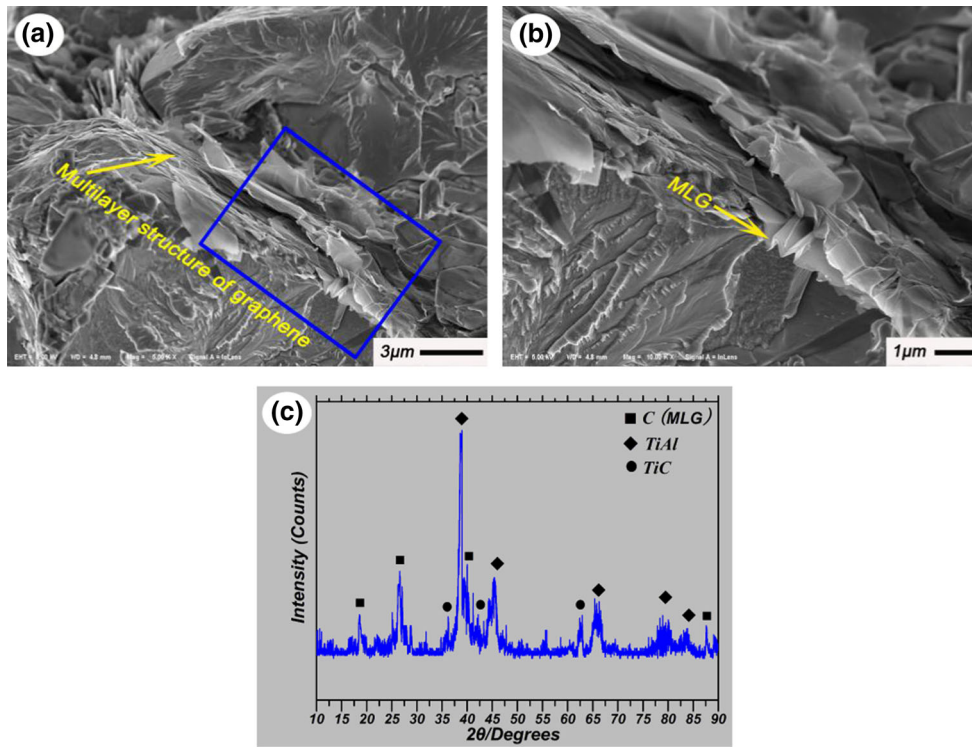
Fig. 4 Typical FESEM image of MLG in the cross section of TCM (a), magnified micro-morphology of local region marked by rectangle in (b) and XRD pattern (c) of γ-TiAl-1.75 wt.% MLG
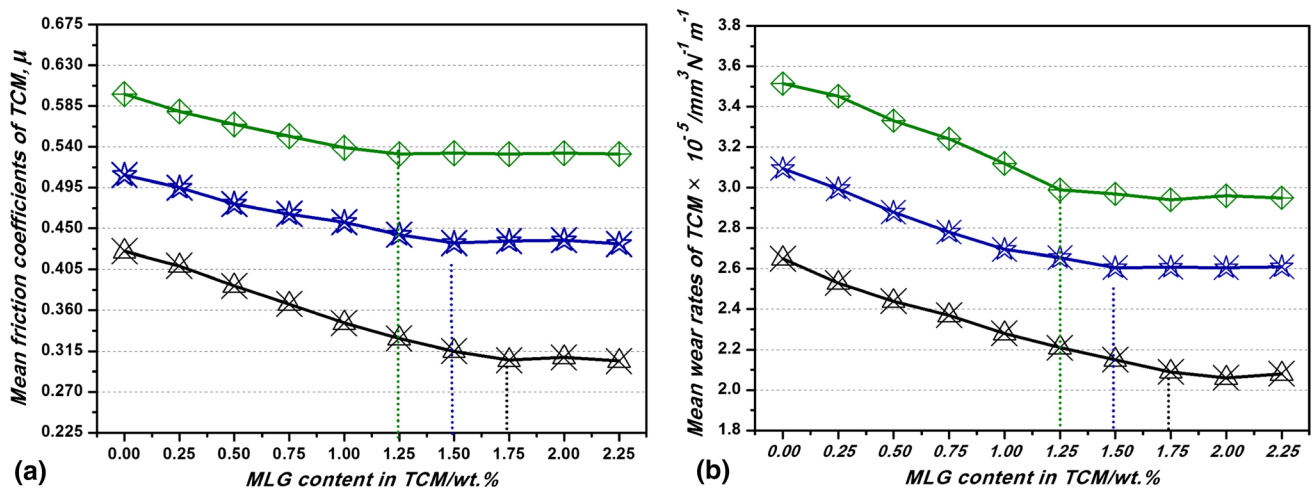

Fig. 5 Representative mean friction coefficients (a) and wear rates (b) of TCM after dry sliding process

increase in addition amounts of MLG at different applied loads, such as 1.25 wt.% MLG at 4 N, 1.50 wt.% MLG at 8 N and 1.75 wt.% MLG at 12 N. In particular, the excellent tribological behavior of γ-TiAl-1.75 wt.% MLG with the small friction coefficient of 0.31 and less wear rate of 2.09×10^{-5} mm^3 N^{-1} m^{-1} is obtained at 12 N. It may be attributed to the thickness of friction layer and high nano-hardness under the action of continuous extrusion stress and cyclic shear stress during early stages of sliding friction.

3.2 Effect of MLG on Nano-Hardness of TCM

3.2.1 Effect of MLG Content on Nano-Hardness. Figure 6(a) exhibits the typical three load-depth plots of nano-indentation in γ-TiAl-1.75 wt.% MLG. Figure 6(b) shows the mean nano-hardness of TCM after three tests. As shown in Fig. 6, the mean nano-hardness of TCM is improved up to 9.03 GPa from 6.20 GPa with the increasing of MLG addition amounts (0-1.75 wt.%) and reaches up to the values of 9.03-
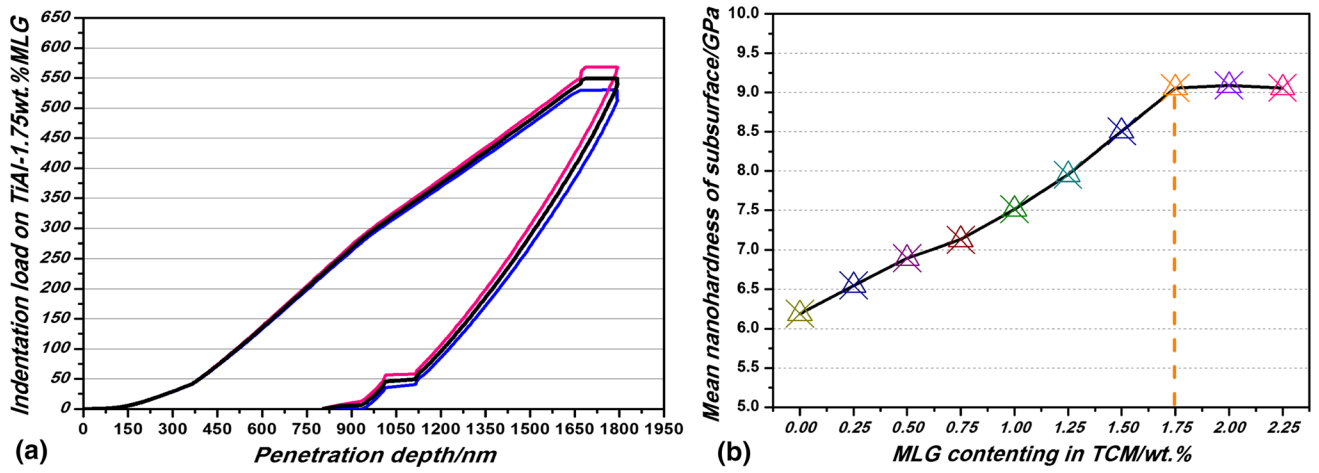
Fig. 6 Typical three load-depth plots of nano-indentations in γ-TiAl-1.75 wt.% MLG (a) and mean nano-hardness of TCM after three tests (b) under a load of 12 N
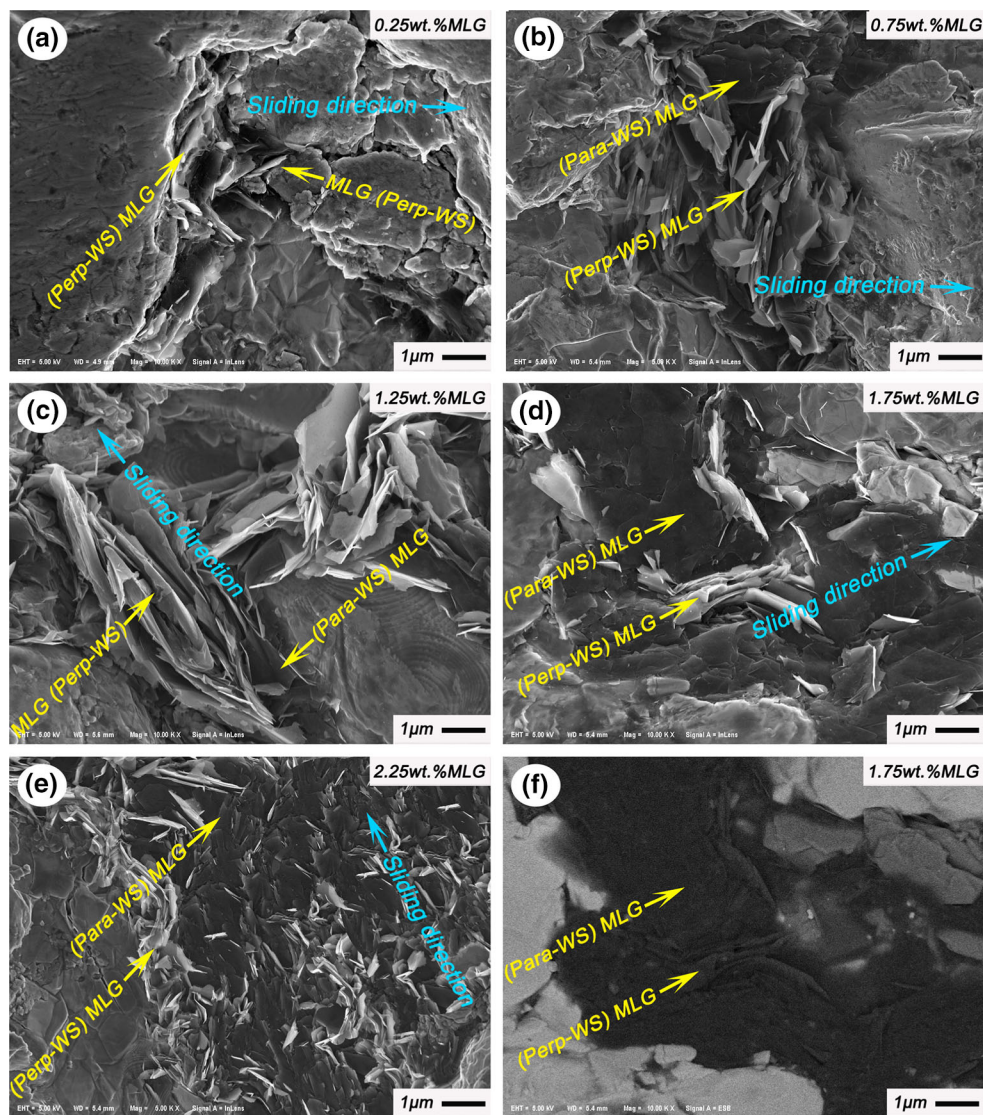

Fig. 7 Representative FESEM morphologies of wear scars of TCM at 12 N (a-e) and back-scattered image of wear scar of γ-TiAl-1.75 wt.% MLG (f)

9.06 GPa with the addition amounts of 1.75-2.25 wt.% MLG. Obviously, the nano-hardness of γ-TiAl-1.75 MLG reaches a relatively stable value of 9.03 GPa at 12 N.

3.2.2 Effect of Distribution and State of MLG on Nano-Hardness. Figure 7(a) and (e) exhibits the representative FESEM morphologies of wear tracks of TCM at 12 N. As shown in Fig. 7(a) and (d), when the addition amount of MLG increases up to 1.75 wt.% from 0.25 wt.%, the distribution of MLG on wear scar is gradually improved after sliding test, and the main existing status of MLG is gradually transformed into Para-WS from Perp-WS. As shown in Fig. 7(e), when the addition amount of MLG is 2.25 wt.%, most of Perp-WS MLG on the worn surface of TCM is easily scaled off to form wear debris, which are easy to be taken away by Si_3N_4 balls. In consequence of the existing of low bonding force between layer and layer, the nano-indentation hardness of Para-WS MLG is higher than that of Perp-WS MLG. Hence, the appropriate distribution of MLG on wear scar and the transformation of main existence status (from Perp-WS to Para-WS) lead to the gradually improving of mean nano-hardness (see Fig. 6b).

Figure 7(f) exhibits the typical back-scattered image of wear scar of γ-TiAl-1.75 wt.% MLG. As shown in Fig. 7(f), MLG is distributed on wear scar of γ-TiAl-1.75 wt.% MLG along the direction of Para-WS, leading to a friction-reducing and an increase in wear resistance of the composites.

3.2.3 Influence of Nano-Hardness on Tribological Behavior of TCM. As shown in Fig. 5 and 6(b), it can be found that the increasing of addition amounts of MLG (0-1.75 wt.%) is beneficial to the improvement of nano-hardness (6.19-9.03 GPa), leading to the decrease in friction coefficients (0.43-0.31) and wear rates (2.65-2.09 × 10^{-5} mm^3 N^{-1} m^{-1}). As the addition amount of MLG increases up to 2.25 wt.% from 1.75 wt.% at 12 N, the mean nano-hardness of γ-TiAl-1.75 wt.% MLG reaches up to the values of 9.03-9.06 GPa, leading to the acquiring of small friction coefficients of 0.30-0.31 and less wear rates of 2.08-2.09 × 10^{-5} mm^3 N^{-1} m^{-1}. The nano-hardness is higher than that of the original substrate of the composites, which in turn can prevent the hard protrusions of Si_3N_4 ball from being pressed into the substrate, thereby reducing the plastic deformation such as the deep furrows and
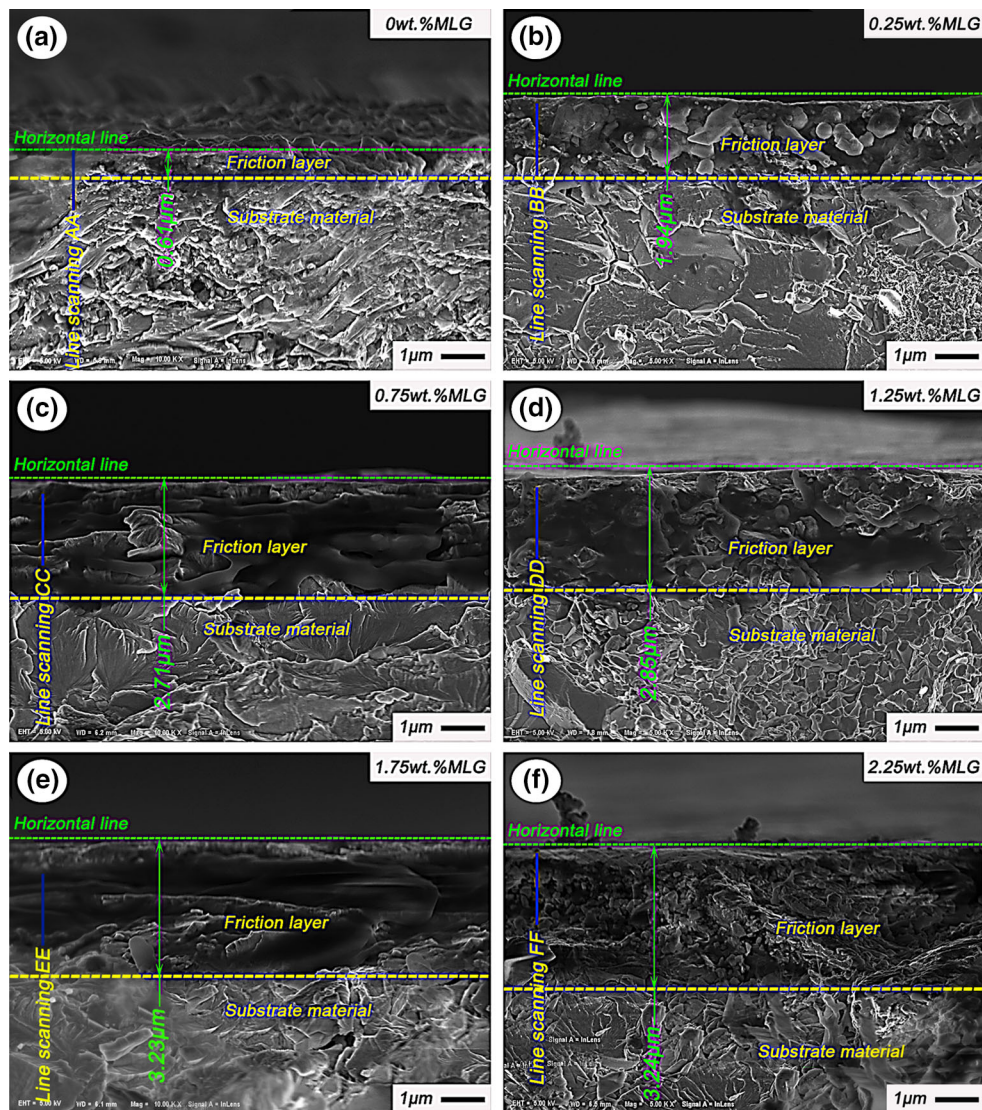

Fig. 8 Typical FESEM morphologies of cross sections of worn surfaces of TCM with different amounts of MLG under a load of 12 N: 0 wt.% (a), 0.25 wt.% (b), 0.75 wt.% (c), 1.25 wt.% (d), 1.75 wt.% (e) and 2.25 wt.% (f)

scratches formed at the effect of cyclic shear strain. It is similar to previous studies that the friction coefficient μ and wear rate W of composites are continuously lowered with the increase in nano-hardness (Ref 18, 19).

3.3 Influence of Friction Layer Thickness on Tribological Behavior of TCM

Figure 8 exhibits the typical FESEM morphologies of cross sections of worn surfaces of TCM obtained after tests under a load of 12 N. As shown in Fig. 8(a) and (e), the friction layer thickness obtained after 80 min sliding increases up to 3.23 μm from 0.61 μm with the increasing of addition amounts of 0-1.75 wt.% MLG. When the addition amount of MLG is in the region of 1.75-2.25 wt.%, the friction layer thickness is close to the value of 3.23-3.24 μm as shown in Fig. 8(e) and (f). It demonstrates that the thickness of friction layer underneath the worn surface of γ-TiAl-1.75 wt.% MLG obtains a relatively stable value of 3.23 μm after dry sliding wear test. MLG in thick friction layer increases the capacity for resisting deformation and enhances the fracture toughness and flexural strength of the composites. Hence, it is hard to remove materials from worn surface of γ-TiAl-1.75 wt.% MLG with thick friction layer during the process of adhesive and abrasive wear.

3.4 The Combined Effects of Friction Layer Thickness and Nano-Hardness on Tribological Behavior of TCM

According to the above analysis, it can be concluded that the friction coefficients and wear rates of TCM are continually lowered with the increase in friction layer thickness h and subsurface nano-hardness H. The main existence status of Para-WS and the distribution of MLG as well as appropriate MLG content in friction layer result in the high mean nano-hardness of γ-TiAl-1.75 wt.% MLG under a load of 12 N. Additionally, under the action of continuous extrusion stress and due to the circular sliding of Si_3N_4 counterface ball in the same wear track, a continuous and thick friction layer is formed, which provides the low-strength junctions at the interface, significantly reducing the friction coefficient and wear rate of TCM during the sliding process.

4. Conclusions

In order to acquire an understanding of the friction and wear mechanisms of TCM containing varied contents of MLG, the tribological performance of TCM against Si_3N_4 counterface is investigated in a range of applied loads from 4 to 12 N with a constant speed of 0.2 m/s at ambient temperature of 25 °C.

It can be concluded that the main existence status of Para-WS and the distribution of MLG as well as appropriate MLG content in friction layer result in the high mean nano-hardness of γ-TiAl-1.75 wt.% MLG under a load of 12 N. The high nano-hardness leads to the increase in resisting plastic deformation capacity and reduces the material loss. Moreover, under the action of continuous extrusion stress and due to the circular sliding of Si_3N_4 counterface balls on the same wear track, a continuous and thick friction layer is formed, which provides the low-strength junctions at the interface, significantly reducing the friction coefficient and wear rate of TCM during the sliding process.

It is also observed that MLG in TCM makes contributions to the formation of the thick friction layer. Meanwhile, MLG, which has the properties of high tensile strength and being easily sheared off, accumulates in friction layer and tends to be parallel to the worn surface, leading to the increase in friction reduction and wear resistance of TCM. Furthermore, γ-TiAl-1.75 wt.% MLG obtained the smaller friction coefficient of 0.31 and less wear rate of 2.09×10^{-5} mm^3 N^{-1} m^{-1} at 12 N.

References

1. J. Cheng, Y. Yu, L.C. Fu, and F. Li, Effect of TiB$_2$ on Dry-Sliding Tribological Properties of TiAl Intermetallics, *Tribol. Int.*, 2013, **62**, p 91–99
2. Z.S. Xu, X.L. Shi, W.Z. Zhai, M. Wang, Z.W. Zhu, and J. Yao, Preparation and Tribological Properties of TiAl Matrix Composites Reinforced by Multilayer Graphene, *Carbon*, 2014, **67**, p 168–177
3. J.S. Lin, L.W. Wang, and G.H. Chen, Modification of Graphene Platelets and their Tribological Properties as a Lubricant Additive, *Tribol. Lett.*, 2011, **4**, p 209–215
4. Y.Y. Zhang, C.M. Wang, Y. Cheng, and Y. Xiang, Mechanical Properties of Bilayer Graphene Sheets Coupled by sp3 Bonding, *Carbon*, 2011, **49**, p 4511–4517
5. J.W. Suk, R.D. Piner, and J. An, Mechanical Properties of Monolayer Graphene Oxide, *ACS Nano*, 2010, **4**, p 6557–6564
6. S. Ghosh, I. Calizo, D. Teweldebrhan, E.P. Pokatilov, and L. Nika, Extremely High Thermal Conductivity of Graphene: Prospects for Thermal Management Applications in Nanoelectronic Circuits, *Appl. Phys. Lett.*, 2008, **92**, p 151911–151913
7. R. Prasher, Graphene Spreads the Heat, *Science*, 2010, **328**, p 185–186
8. J. Yao, X.L. Shi, W.Z. Zhai, A.M.M. Ibrahim, Z.S. Xu, L. Chen, Q.S. Zhu, Y.C. Xiao, Q.X. Zhang, and Z.H. Wang, The Enhanced Tribological Properties of NiAl Intermetallics: Combined Lubrication of Multilayer Graphene and WS$_2$, *Tribol. Lett.*, 2014, **56**, p 573–582
9. K. Yang, X.L. Shi, and W.Z. Zhai, Tribological Behavior of TiAl Matrix Self-Lubricating Composites Reinforced by Multilayer Graphene, *Rsc. Adv.*, 2015, **5**(55), p 44618–44625
10. Z.S. Xu, L. Chen, X.L. Shi, Q.X. Zhang, A.M.M. Ibrahim, W.Z. Zhai, J. Yao, Q.S. Zhu, and Y.C. Xiao, Formation of Friction Layers in Graphene-Reinforced TiAl Matrix Self-Lubricating Composites, *Tribol. Trans.*, 2015, **58**(4), p 668–678
11. A. Moshkovich, V. Perfilyev, T. Bendikov, I. Lapsker, H. Cohen, and L. Rapoport, Structural Evolution in Copper Layers During Sliding Under Different Lubricant Conditions, *Acta Mater.*, 2010, **58**(14), p 4685–4692
12. W.Z. Zhai, X.L. Shi, Z.S. Xu, and Q.X. Zhang, Formation of Friction Layer of Ni$_3$Al Matrix Composites with Micro- and Nano-Structure During Sliding Friction Under Different Loads, *Mater. Chem. Phys.*, 2014, **147**(3), p 850–859
13. A. Nieto, D. Lahiri, and A. Agarwal, Synthesis and Properties of Bulk Graphene Nanoplatelets Consolidated by Spark Plasma Sintering, *Carbon*, 2012, **50**, p 4068–4077
14. American Society for Testing and Materials, Standard Test Method for Vickers Hardness of Metallic Materials. ASTM E92-82; e2 2003
15. American Society for Testing and Materials, Standard Test Methods for Density of Compacted or Sintered Powder Metallurgy (PM) Products Using Archimedes' Principle. ASTM B962-08; 2008

16. American Society for Testing and Materials, Standard Test Method for Wear Testing With a Pin-On-Disk Apparatus. ASTM G99-05; 2010

17. R.D. Tyagi, S. Xiong, and J.L. Li, Effect of Load and Sliding Speed on Friction and Wear Behavior of Silver/h-BN Containing Ni-base P/M Composites, *Wear*, 2011, **270**, p 423–430

18. B.B. Bhushan, Ge. Shirong, Introduction to Tribology, China Machine Press, 2006, p 08

19. I. Ahmad, A. Kennedy, and Y.Q. Zhu, Wear Resistant Properties of Multi-Walled Carbon Nanotubes Reinforced Al_2O_3 Nanocomposites, *Wear*, 2010, **269**, p 71–78